

Influence of Intrachain Hydrogen Bonding on the Cyclization of a Polystyrene Chain

J. P. S. FARINHA,¹ J. M. G. MARTINHO,^{1,*} H. XU,² M. A. WINNIK,² and R. P. QUIRK³

¹Centro de Química-Física Molecular, Instituto Superior Técnico, 1096 Lisboa Codex, Portugal;

²Department of Chemistry and Erindale College, University of Toronto, Toronto, Ontario, Canada M5S 1A1;

³Department of Polymer Science, University of Akron, Akron, Ohio 44325

SYNOPSIS

Cyclization of a polystyrene chain ($M_n = 10,600$; $M_w/M_n = 1.09$) both ends labeled with 4-(1-pyrenyl)butanoamide groups was studied in cyclohexane between 25 and 95°C. The amide groups (peptide bonds) at both ends can form an intrachain hydrogen bond between the amide hydrogen at one chain end and the carbonyl oxygen at the other. The presence of two sets of conformers, random coils, and chains cyclized through hydrogen bonding, complicates the data analysis. The pyrene excimer kinetics of this polymer is well described by a model composed of two monomers (hydrogen bonded and nonbonded chains) and one excimer, in equilibrium. The cyclization rate constant for hydrogen-bonded chains is larger than the one for nonhydrogen-bonded chains. The pyrene excimer binding energy (ca. 1.6 kcal/mol) is lower than the published value for nonhydrogen-bonded chains (~ 9 kcal/mol), suggesting that intrachain hydrogen bonding hinders the stabilization of the excimer. © 1994 John Wiley & Sons, Inc.

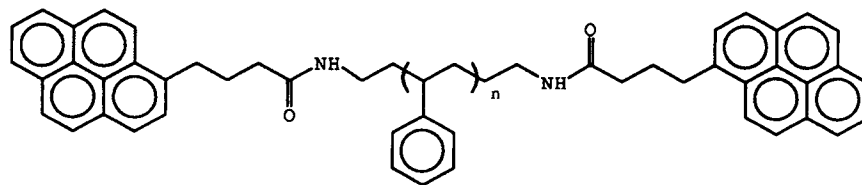
Keywords: cyclization • fluorescence • polystyrene • hydrogen bonding

INTRODUCTION

Pyrene forms excimers (excited dimers) in solution, on the encounter of an electronic excited pyrene molecule with a ground state molecule.¹ This process is diffusion-controlled and because of that has been used as a tool in the polymer field, furnishing rele-

vant information on the conformation and dynamics of polymer chains.² Some of the most interesting experiments were done with polymer chains with fluorophores attached at both ends or distributed along the chain backbone.^{2,3}

Here we present the case of the polystyrene derivative, referred to as polymer (I), labeled at both ends with a 4-(1-pyrenyl)butanoamide molecule.



Polymer I

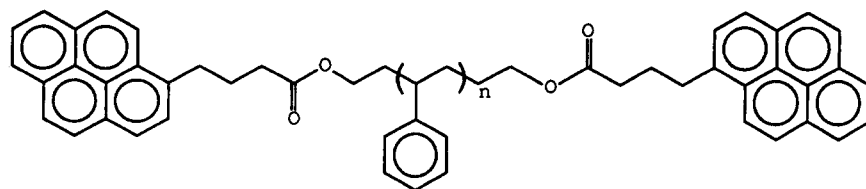
Polymer I was prepared from a sample of bis-amino end-capped polystyrene, purified by column chromatography to ensure the presence of two amino

groups per chain. Owing to the presence of amide groups at both chain ends, intrachain hydrogen bonding between the amide hydrogen at one end and the oxygen of the carbonyl at the other ($\text{>N-H} \cdots \text{O}=\text{C}<$) is possible. The hydrogen bonds are similar to the ones observed, for instance,

* To whom correspondence should be addressed.

in proteins and Nylon, giving particularly interesting properties to these molecules. The intrachain hydrogen bond in polymer I promotes the close approach of the two chain ends, disturbing the chain-end distance distribution function (Gaussian in θ solvents).

The excitation spectra of dilute solutions of polymer I recorded at the pyrene monomer and excimer emissions are different, suggesting the formation of ground-state pyrene dimers. By contrast, pyrene monomer and excimer emissions for polymer II, where ground-state aggregation is very small, show identical excitation spectra.



Polymer II

The fluorescence decay curves of diluted solutions of polymer I cannot be described by a two-state monomer–excimer model (Birks' kinetics). On the other hand, a three-state model composed of two monomers and one excimer, describes reasonably well both pyrene monomer and excimer decay curves. The monomers are associated with hydrogen-bonded and nonbonded chains. Analysis of the pyrene monomer and excimer decay curves obtained at several temperatures allow the determination of all the relevant kinetic parameters, namely the cyclization rate constants for both monomers. The cyclization rate constant is higher for hydrogen-bonded chains than for nonhydrogen-bonded chains. This results from differences between the chain-ends distance distribution functions of the two monomers. The excimer binding energy (~ 1.6 kcal/mol) is rather small and is lower than the published values for both intermolecular^{1,4} and intramolecular pyrene excimers of chains of structure II (ca. 9 kcal/mol).⁵ We interpret this to mean that there are steric constraints to attainment of a proper excimer geometry caused by the intrachain hydrogen bond.

SAMPLE PREPARATION AND EXPERIMENTAL SETUP

Polystyrene chain I was labeled with 4-(1-pyrenyl)butanoamide groups at both ends, from a polystyrene chain end terminated with NH_2 groups. The polymer chain was synthesized by anionic polymerization following standard procedures, described elsewhere.⁶ The labeling process was carried out by treating the NH_2 -terminated polymer with excess 4-(1-pyrene)butyryl chloride in toluene/triethylamine. After the reaction, the mixture was filtered and precipitated into methanol. The polymer was

then dissolved in tetrahydrofuran (THF) and purified further by preparative gel permeation chromatography (GPC). The purity of the polymer was checked by GPC using both the ultraviolet visible (UV-Vis) and fluorescence detectors. A monodisperse polymer sample ($M_n = 10,600$; $M_w/M_n = 1.09$) with both ends labeled (structure I) was obtained. The percentage of labeling calculated by UV-Vis absorption using the methyl ester of pyrenebutyric acid in toluene as a model compound [$\epsilon(345 \text{ nm}) = 3.83 \times 10^4 \text{ M}^{-1} \text{ cm}^{-1}$] was around 95%. Polymer II ($M_n = 2600$; $M_w/M_n = 1.08$) was synthesized and labeled as described in ref. 2c.

Spectroscopic grade quality cyclohexane, toluene, and dimethylformamide from Merck, were used as received. Solutions of polymers I and II (ca. $2 \times 10^{-6} \text{ M}$) were degassed using the freeze-pump-thaw technique and sealed under a vacuum better than 2×10^{-5} bar. Fluorescence measurements were made at constant temperature ($\pm 0.5^\circ\text{C}$) between 25 and 95°C . Fluorescence spectra were recorded on a Spex Fluorolog 112 spectrofluorometer. Decay curves were obtained by the single photon timing technique and were analyzed using an iterative reconvolution method based on the algorithm of Marquard.⁷ The excitation light ($\lambda = 337 \text{ nm}$), from a coaxial flash lamp (Edinburg Instruments, Model 199f) was selected by a Jobin-Yvon (model H-20) monochromator. The monomer fluorescence ($\lambda = 376 \text{ nm}$) and the excimer fluorescence ($\lambda = 520 \text{ nm}$) were selected by a Jobin-Yvon (model H-20) monochromator and detected by a Philips XP2020Q photomultiplier. In order to eliminate the color shift of the photomultiplier, the delta pulse convolution technique was used.⁸ Reference decay curves of diluted solutions of 1,4-bis(5-phenyl-1,3-oxazol-2-yl)benzene (POPOP) in cyclohexane ($\tau = 1.1 \text{ ns}$)

and 2,5-bis(5-ter-butyl-2-benzoxazolyl)thiophene (BBOT) in 95% ethanol ($\tau = 1.47$ ns) were used in the analysis of pyrene monomer and excimer decay curves, respectively.

RESULTS

Fluorescence Spectra

Fluorescence spectra of dilute (2×10^{-6} M) solutions of polymers **I** and **II** are composed of two well-separated bands. A structured one, characteristic of the pyrene monomer emission in the blue, and a broader one at longer wavelength (centered around 480 nm), characteristic of the excimer emission. This indicates that upon pyrene electronic excitation the polystyrene chain cyclizes with the formation of a pyrene excimer. The pyrene fluorescence spectrum of a dilute solution (ca. 2×10^{-6} M) of polymer **I** excited at 345 and 355 nm is presented in Figure 1. The first monomer emission peak was used to normalize both spectra.

The excimer intensity is higher for excitation at 355 nm where the pyrene monomer molar absorptivity is very small. This suggests that ground-state pyrene dimers are formed, otherwise the monomer-to-excimer pyrene fluorescence intensities ratio should be independent of excitation wavelength. Under usual circumstances, when the excimer's ground state is dissociative, this ratio is constant since the excimer is populated only via the excited

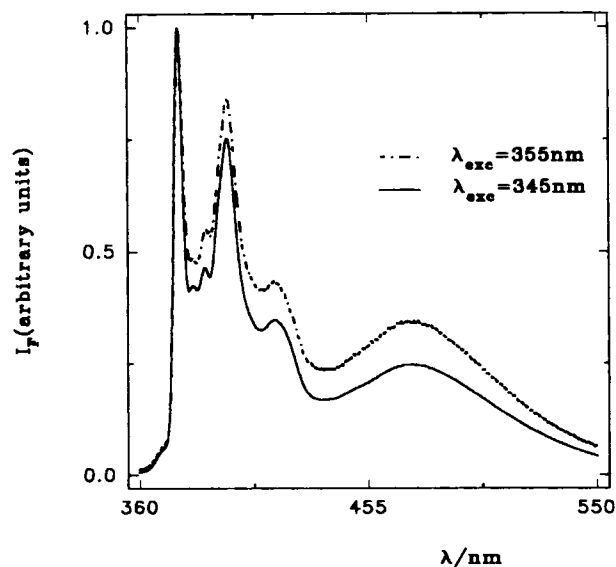


Figure 1. Fluorescence spectra of a 2×10^{-6} M solution of polymer **I** in cyclohexane. (---) $\lambda_{\text{exc}} = 355$ nm; (—) $\lambda_{\text{exc}} = 345$ nm.

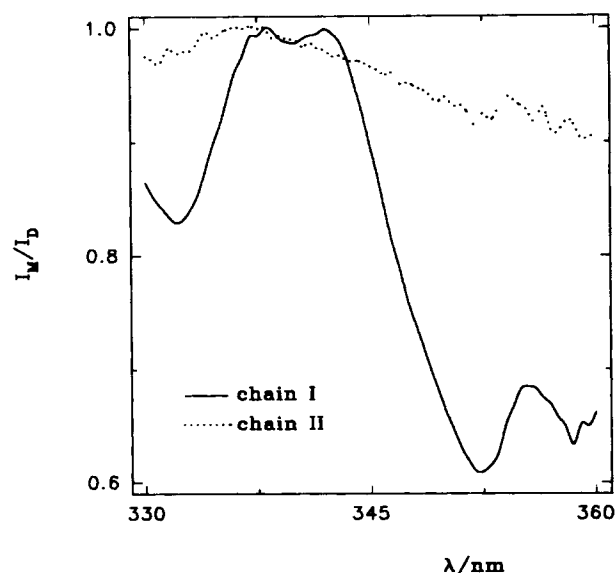


Figure 2. Ratio of the monomer ($\lambda = 376$ nm) to excimer ($\lambda = 520$ nm) fluorescence intensities versus excitation wavelength at 25°C of diluted solutions (2×10^{-6} M) of polymers **I** and **II** in cyclohexane. (—) Polymer **I**; (···) Polymer **II**.

monomer. Figure 2 compares the monomer to excimer pyrene fluorescence intensities (I_M/I_D) of polymers **I** and **II** in cyclohexane. The values were normalized to 1 in the absorption maximum of pyrene monomer ($\lambda = 345$ nm), where a very small percentage of dimer absorption is expected.

The ratio of intensities versus excitation wavelength is practically constant for chain **II** but varies significantly for chain **I**. This suggests that the intrachain hydrogen bonding in chain **I** promotes ground-state pyrene association, owing to the proximity of pyrene chain ends. This is not surprising since, in the last 10 years, ground-state pyrene association was observed in different media, this topic being recently reviewed by F. M. Winnik.⁹

It is well known that intermolecular pyrene excimer is shifted to the red in polar solvents.¹⁰ For the individual polymer chains **I** and **II** the maximum of the excimer band is constant in cyclohexane, dimethylformamide, and toluene. This shows that pyrene excimer solvatochromic shifts are minimal when the excimer is contained within the polymer coil. Nevertheless, the maximum of the excimer spectra for polymer **I** is slightly blue-shifted in all solvents compared to polymer **II** (Fig. 3).

This is not consistent with the lower polarity of the ester group in polymer **II**, probably being due to a less favorable excimer conformation in polymer **I**, owing to the intrachain hydrogen bond.

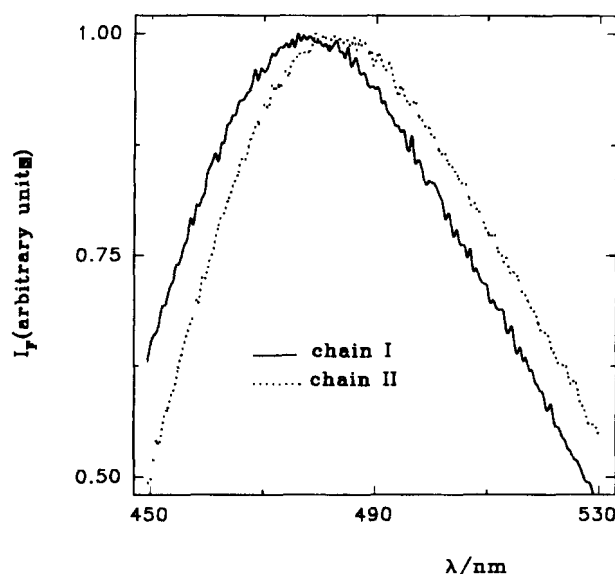


Figure 3. Excimer fluorescence spectra of diluted solutions (2×10^{-6} M) of polymers I and II in cyclohexane. (—) Polymer I; (···) Polymer II.

Kinetic Model

The pyrene monomer and excimer decay curves of chain I in cyclohexane can be fitted only with a sum of three exponentials. Since the two-state Birks' model describes well the excimer formation kinetics in polymer II, we attribute the different behavior of polymer chain I to the presence of an additional subset of ground-state populations.

To describe the excimer kinetics of polymer I, we propose a three-state model comprised of two pyrene monomers (M_1 and M_2) and one pyrene dimer (D). The monomers in equilibrium with constant K_3 are associated with random-coil chains (M_1) and hydrogen-bonded (M_2) chains. Owing to the pyrene chain-end groups both chain conformers (M_1 and M_2) are still in equilibrium with cyclized chains forming a dimer (D) with constants K_4 and K_3K_4 , respectively. Upon electronic excitation the three species in equilibrium can be excited to give the corresponding species M_1^* , M_2^* , and D^* , according to their optical densities.

The excited pyrene monomers (M_1^* and M_2^*) decay with intrinsic decay constant Γ_M , and compete to form excimers with distinct cyclization rate constants k_1 and k_2 , respectively. These values are distinct since each monomer population has a different chain-ends distance distribution function. Once formed, the excimer can decay with intrinsic decay constant Γ_D , or dissociate with rate constant k_d to regenerate both type of excited monomers (M_1^* and

M_2^*). We assume that both excimer dissociation processes have the same rate constant k_d . This is a reasonable assumption since the excimer dissociation is controlled by the excimer binding energy and the chain-ends diffusion, this being almost independent of the intrachain hydrogen bonding. On the other hand, the equilibrium constant between monomers ($K_3 = k_3/k_{-3}$) is assumed to be equal in the ground and excited states, which means that the hydrogen bond is independent of the pyrene excitation energy.

The rate equations can be written in a matrix formulation

$$\frac{d}{dt} \mathbf{X} = \mathbf{K} \mathbf{X} \quad (1)$$

Where \mathbf{X} is the vector of the concentrations and \mathbf{K} the rate matrix.

$$\mathbf{X} = \begin{bmatrix} [M_1^*] \\ [D^*] \\ [M_2^*] \end{bmatrix} \quad \mathbf{K} = \begin{bmatrix} -A & k_d & k_{-3} \\ k_1 & -B & k_2 \\ k_3 & k_d & -C \end{bmatrix} \quad (2)$$

with

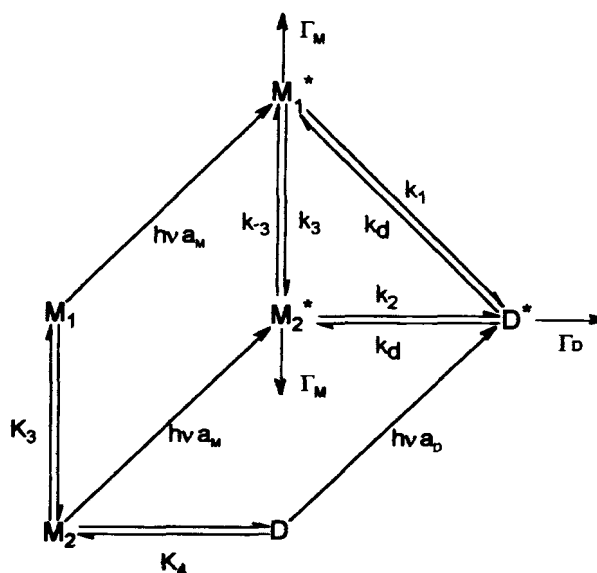
$$A = \Gamma_M + k_1 + k_3 \quad (3a)$$

$$B = \Gamma_D + 2k_d \quad (3b)$$

$$C = \Gamma_M + k_2 + k_{-3} \quad (3c)$$

The solution of eq. (1) is of the form

$$\mathbf{X} = \mathbf{X}_0 \exp(\mathbf{K}t) \quad (4)$$



Scheme 1.

Where \mathbf{X}_0 is the vector of the initial conditions. Using standard procedures,¹¹ the decay constants (λ_i ; $i = 1, 3$) are obtained from the eigenvalue equation

$$\det(\mathbf{K} - \lambda\mathbf{I}) = 0 \quad (5)$$

If the solution of eq. (5) is nondegenerate, eq. (4) can be written,

$$\mathbf{X}(t) = \alpha_1 \mathbf{C}_1^0 \exp(\lambda_1 t) + \alpha_2 \mathbf{C}_2^0 \exp(\lambda_2 t) + \alpha_3 \mathbf{C}_3^0 \exp(\lambda_3 t) \quad (6)$$

where \mathbf{C}_i^0 are arbitrary chosen eigenvectors of \mathbf{K} (associated with λ), obeying the eigenvector equation

$$\mathbf{K}\mathbf{C}_i = \lambda_i \mathbf{C}_i \quad (7)$$

and α_i are scalar constants obtained from the zero-time condition

$$\mathbf{C}^0 \alpha = \mathbf{X}_0 \quad (8)$$

A particular solution \mathbf{C}^0 with matrix columns \mathbf{C}_i^0 , is

$$\mathbf{C}_i^0 = \begin{bmatrix} k_{-3}(B + \lambda_i) + k_2 k_d \\ k_2(A + \lambda_i) + k_{-3} k_1 \\ (A + \lambda_i)(B + \lambda_i) - k_1 k_d \end{bmatrix} \quad (9)$$

and the corresponding α_i obtained from eq. (8), are

$$\alpha_i = [\mathbf{M}_i^*]^0 \alpha'_i \quad (10)$$

where the concentration of initially excited M_1 is

$$[\mathbf{M}_i^*]^0 = a_M \frac{1}{1 + K_3 + K_4} C_0 \quad (11)$$

being C_0 the concentration of polymer, a_M the relative molar absorptivity of M_1

$$a_M = \frac{\epsilon_M}{2\epsilon_M + \epsilon_D} \quad (12)$$

and ϵ_M , ϵ_D the molar absorptivities of the pyrene monomer ($\epsilon_{M_1} = \epsilon_{M_2}$) and the dimer, respectively. The values of α'_i are given by

$$\alpha'_1 = \frac{1 - c_{31}^0 \alpha'_3 - c_{21}^0 \alpha'_2}{c_{11}^0} \quad (13a)$$

$$\alpha'_2 = - \frac{\alpha'_3 \theta_2 + c_{12}^0 - c_{11}^0 K'_4}{\theta_3} \quad (13b)$$

$$\alpha'_3 = \frac{(c_{11}^0 K_3 - c_{13}^0) \theta_3 + (c_{11}^0 K_3 K'_4 - c_{12}^0) \theta_4}{\theta_1 \theta_3 + \theta_2 \theta_4} \quad (13c)$$

with

$$\theta_1 = c_{11}^0 c_{22}^0 - c_{12}^0 c_{21}^0 \quad (14a)$$

$$\theta_2 = c_{13}^0 c_{21}^0 - c_{11}^0 c_{23}^0 \quad (14b)$$

$$\theta_3 = c_{11}^0 c_{33}^0 - c_{13}^0 c_{31}^0 \quad (14c)$$

$$\theta_4 = c_{11}^0 c_{32}^0 - c_{12}^0 c_{31}^0 \quad (14d)$$

and the apparent equilibrium constant

$$K'_4 = \frac{\epsilon_D}{\epsilon_M} K_4 \quad (15)$$

Decay Curve Measurements

From the analysis of pyrene monomer and excimer decay curves three lifetimes ($\tau_i = -1/\lambda_i$, $i = 1, 3$) and four pre-exponential factors ratios

$$\frac{a_1^M}{a_2^M} = \frac{\alpha_1 (c_{11}^0 + c_{13}^0)}{\alpha_2 (c_{21}^0 + c_{23}^0)} \quad (16a)$$

$$\frac{a_1^M}{a_3^M} = \frac{\alpha_1 (c_{11}^0 + c_{13}^0)}{\alpha_3 (c_{31}^0 + c_{33}^0)} \quad (16b)$$

$$\frac{a_1^D}{a_2^D} = \frac{\alpha_1 c_{12}^0}{\alpha_2 c_{22}^0} \quad (16c)$$

$$\frac{a_1^D}{a_3^D} = \frac{\alpha_1 c_{12}^0}{\alpha_3 c_{32}^0} \quad (16d)$$

can be obtained which allow the evaluation of seven model parameters (k_3 ; k_{-3} ; K'_4 ; Γ_D ; k_1 ; k_2 ; and k_d). However, the evaluation is difficult since no analytical solution exists for the model parameters versus the fitted parameters, and the application of standard numerical methods of minimization is not appropriate. So a coarse grid mapping of the parameter space was initially done in order to locate the main minima and identify the desired range of parameters over which the search was refined. This was done dividing the probable range for each parameter p_j in a number n_j of equal increments so that the parameter space was divided in $\prod_{j=1}^7 n_j$ hy-

percubes. The χ^2 was evaluated at the vertices of these hypercubes and interactively minimized in a DEC-VAX 9000 computer to obtain the best parameters.

Figures 4 and 5 show pyrene monomer and excimer fluorescence decay curves of polymer I solutions in cyclohexane at 25°C.

The excimer decay curve was fitted with a sum of three exponentials being the lifetimes at 25°C $\tau_1 = 14$ ns, $\tau_2 = 67$ ns, $\tau_3 = 170$ ns, and the sum of pre-exponential factors different from zero. This sum remains different from zero for the full range of temperatures, showing that pyrene dimers are formed. The monomer fluorescence can be fitted only with a sum of four exponentials, with one of the lifetimes close to that for the decay of chains containing only one pyrene group. Constraining one of the lifetimes to the value obtained from the single-exponential decay curve of one-end-labeled chains ($\tau_4 = 318$ ns for 25°C), decay times $\tau_1 = 14$ ns, $\tau_2 = 67$ ns, $\tau_3 = 171$ ns, where obtained at 25°C. To improve the recovering of the pre-exponential factors, the three excimer decay times plus τ_4 , where then constrained in the monomer decay fit. The four pre-exponential factors of the monomer decays allow the calculation of an amount of 3% of one-end-labeled chains.¹² This value is similar to the value obtained from UV-Vis absorption (see Experimental).

Figure 6 shows the van't Hoff plot of the equilibrium constants K_3 and K'_4 .

The small variation of K_3 with temperature ($\Delta H^0 = -0.7$ kcal/mol) is due to the decrease of the number of intrachain hydrogen bonds with temperature increase. The small increase of K'_4 with temperature

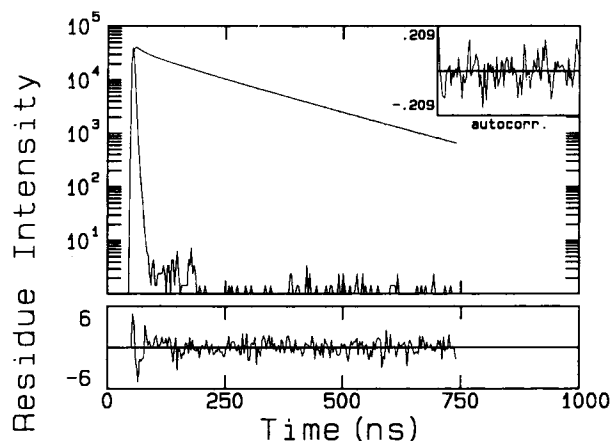


Figure 4. Monomer decay curve of a solution (2×10^{-6} M) of polymer I in cyclohexane at 25°C. $a_1 = 0.05$; $\tau_1 = 14$ ns; $a_2 = 0.02$; $\tau_2 = 67$ ns; $a_3 = 0.13$; $\tau_3 = 171$ ns; $a_4 = 0.003$; $\tau_4 = 318$ ns; $\chi^2 = 1.5$.

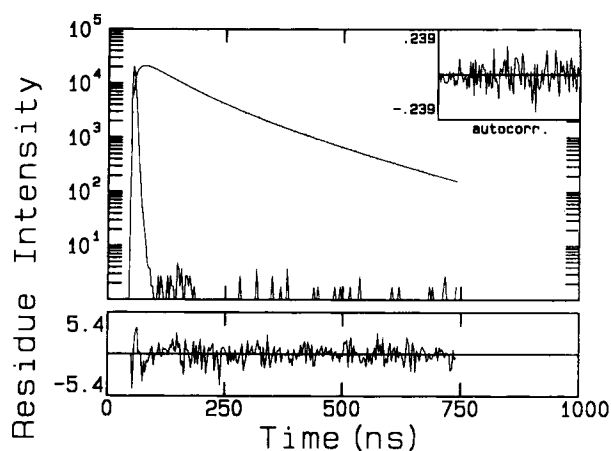


Figure 5. Excimer decay curve of a solution (2×10^{-6} M) of polymer I in cyclohexane at 25°C. $a_1 = -0.23$; $\tau_1 = 14$ ns; $a_2 = 0.25$; $\tau_2 = 67$ ns; $a_3 = 0.09$; $\tau_3 = 170$ ns; $\chi^2 = 1.2$.

means that the equilibrium constant between cyclized chains with and without hydrogen bonds have a positive, close to zero enthalpy, provided the monomer-to-dimer molar absorptivities ratio is temperature invariant. This is reasonable since the pyrene dimer binding energy should be lower than the hydrogen bond energy. Consequently, the equilibrium constant between open chain monomer and dimer ($K_3K'_4$) slightly decreases with temperature.

Figure 7 show the Arrhenius plot of the cyclization rate constants k_1 and k_2 .

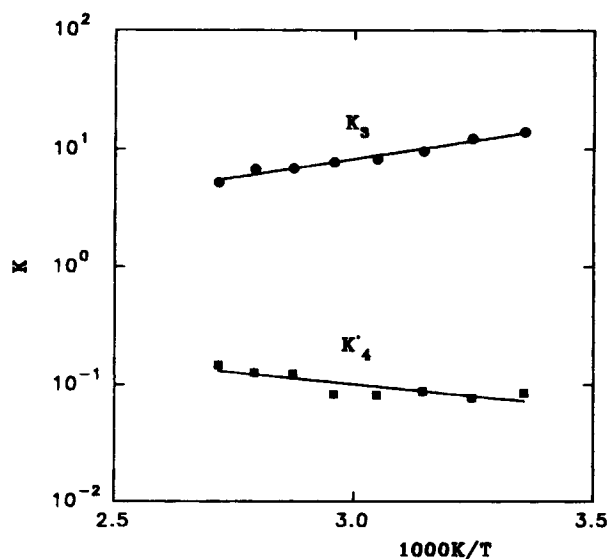


Figure 6. Van't Hoff plot of the cyclization equilibrium constants of polymer I in cyclohexane. (●) for nonhydrogen-bonded chains; (■) for hydrogen-bonded chains (apparent equilibrium constant).

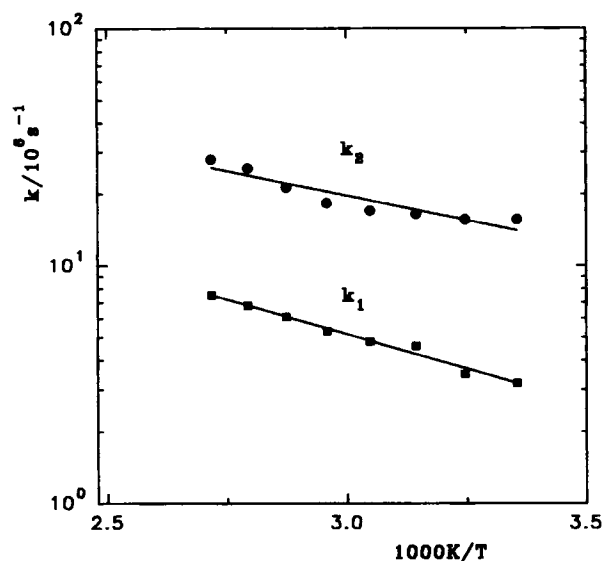


Figure 7. Arrhenius plot of the cyclization rate constants of polymer I in cyclohexane. (●) for hydrogen-bonded chains; (■) for nonhydrogen-bonded chains.

The value of $k_1 = 3.5 \times 10^6 \text{ s}^{-1}$ at 35°C compare well with the value of $4.2 \times 10^6 \text{ s}^{-1}$ obtained for a polymer with the structure of chain II and $M_n = 9200$, at 34.5°C .² The difference between these values can be attributed to the higher molecular weight of polymer I ($M_n = 10600$). The values of k_2 are practically one order of magnitude higher than k_1 , essentially due to smaller average chain-end distance for intrachain hydrogen-bonded chains. Activation energies $E_1 = 2.7 \text{ kcal/mol}$ and $E_2 = 1.9 \text{ kcal/mol}$ were calculated from the plots in Figure 7. The activation energy of k_1 is similar to the activation energy for the cyclization rate constant of polymer II, both being practically equal to the viscous flow activation energy ($E_\eta = 2.9 \text{ kcal/mol}$). The activation energy for k_2 is lower indicating that the dynamics of the cyclization processes is different. Indeed, k_1 depends on the Rouse-Zimm relaxation modes of the chain,¹³ while k_2 should depend on the highly constrained diffusion of the anchored chain ends.

Figure 8 shows the Arrhenius plots for the dissociation rate coefficient, k_d .

The excimer dissociation rate constants for polymer I are one order of magnitude larger than the corresponding ones for polymer II. This suggests a lower pyrene excimer binding energy for polymer I. From the plot of Figure 8, an activation energy, $E_d = 3.5 \text{ kcal/mol}$ was obtained. This value is lower than the pyrene excimer binding energy for polymer II ($\Delta H \approx 9 \text{ kcal/mol}$) which is similar to the values

obtained for the intermolecular pyrene excimer.⁴ Pyrene excimer binding energy of polymer I should still be lower than 3.5 kcal/mol , since this value contains the contribution of the activation energy of the chain ends diffusion process. Considering that the activation energy is equal to E_2 (activation energy of the hydrogen-bonded chains), a very small binding energy of 1.6 kcal/mol is obtained. This suggests that in the ground state, the polymers exist in two conformational states, random coils and chains cyclized through hydrogen bonding. Both sets of polymers form excimers upon electronic excitation. Since the chain ends are together in the excimer state, it is likely that all cyclized random coils are hydrogen bonded during the excimer lifetime.

CONCLUSIONS

The cyclization of polymer I is well described by a three-species kinetic scheme composed of two distinct pyrene monomers and one excimer. The cyclization rate constants of the two monomers are substantially different owing to differences in chain-ends distance distribution functions. Nevertheless, the dynamics should also be different since, on the cyclization of the hydrogen-bonded chain only the diffusion of the chain ends is relevant, while for nonhydrogen-bonded chain the dynamics of the whole chain must be considered. The binding energy of the excimer is very low indicating an unfavorable excimer conformation.

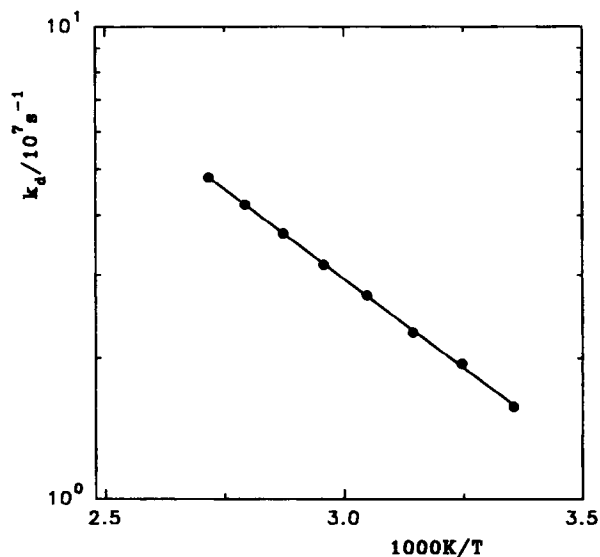


Figure 8. Arrhenius plot of the dissociation excimer rate constant of polymer I in cyclohexane.

This work was supported by Junta Nacional de Investigação Científica e Tecnológica (JNICT) project JNICT/STRDA/P/CEN/421/92 and by NSERC Canada. J. M. G. Martinho acknowledges a fellowship from INVOTAN.

REFERENCES AND NOTES

1. J. B. Birks, *Photophysics of Aromatic Molecules*, John Wiley, New York, 1971.
2. M. A. Winnik, A. E. C. Redpath, K. Panton, and J. Danhelka, *Polymer*, **25**, 91 (1984); J. M. G. Martinho, M. H. Martinho, M. A. Winnik, and G. Beinert, *Makromol. Chem.* **15** (Suppl.), 113 (1989).
3. M. A. Winnik, in *Photophysical and Photochemical Tools in Polymer Science: Conformation, Dynamics, Morphology*, M. A. Winnik (ed.), NATO ASI Series, Reidel, Dordrecht, 1986; M. A. Winnik, *Acc. Chem. Res.*, **18**, 73 (1985).
4. B. Stevens, *Adv. Photochem.*, **8**, 161 (1971); J. M. G. Martinho, J. P. S. Farinha, M. N. Berberan-Santos, J. Duhamel, and M. A. Winnik, *J. Chem. Phys.*, **96**, 8143 (1992).
5. M. A. Winnik, A. E. C. Redpath, and D. H. Richards, *Macromolecules*, **13**, 328 (1980); J. M. G. Martinho, T. Reis e Sousa and M. A. Winnik, *Macromolecules*, **26**, 4484 (1993).
6. R. P. Quirk, W. C. Chen, and P. L. Cheng, in *Reactive Oligomers*, F. W. Harris and H. J. Spinelli (eds.), ACS Symposium Series 282, American Chemical Society, Washington, DC, 1984, p. 139.
7. D. W. J. Marquardt, *Soc. Ind. Appl. Math.*, **11**, 431 (1963); P. R. Bevington, *Data Reduction and Error Analysis in the Physical Sciences*, McGraw-Hill, New York, 1969.
8. M. Zuker, A. G. Szabo, L. Bramall, D. T. Krajcarski, and B. Selinger, *Rev. Sci. Instrum.*, **56**, 14 (1985); H. Van der Zegel, M. Boens, D. Daems, and F. C. De Schryver, *Chem. Phys.*, **101**, 311 (1986).
9. F. M. Winnik, *Chem. Rev.*, **93**, 587 (1993).
10. E. M. S. Castanheira and J. M. G. Martinho, *Chem. Phys. Letters*, **185**, 319 (1991).
11. M. N. Berberan-Santos and J. M. G. Martinho, *J. Chem. Ed.*, **67**, 375 (1990).
12. S. Boileau, F. Méchin, J. M. G. Martinho, and M. A. Winnik, *Macromolecules*, **22**, 215 (1989).
13. C. Cuniberti and A. Perico, *Prog. Polym. Sci.*, **10**, 271 (1984).

Received July 21, 1993

Revised December 22, 1993

Accepted February 18, 1994